CHAPTER 5

CFD RESULTS

CHAPTER (5)

CFD RESULTS

5.1. Introduction

In the present work, a numerical simulation of an inline centrifugal pump was performed using ANSYS Fluent software as mentioned earlier in the previous chapter. ANSYS workbench was used to perform these simulations as it links geometry creation, meshing and simulation process. This link existed in the workbench as blocks of Design modeler, meshing, Fluent and Results. The numerical simulation was performed for both modes: pump mode and turbine mode (Pump As Turbine mode). In this chapter the computational model used for both modes is illustrated in details. In addition, the model validation is presented and performance curve (flowrate vs. head) of both modes were obtained numerically and compared with the experimental ones.

5.2. Geometry drawing

The pump three-dimensional geometry files were not supplied by the manufacturer of the pump as it is considered confidential so the geometry was created by measuring the dimensions of the pump different parts. The used pump is shown in Figure (5-1). The dimensions of the impeller and the volute casing were measured in the fluid mechanics laboratory using Vernier caliper measuring tool as the pump was disassembled to take these measurements as shown in Figures (5-2) and (5-3). The geometry created is lacking the exact shape of the pump volute and outlet pipe which is approximated using measuring tools. The three-dimensional geometry of the pump (i.e. Fluid domain) was created using Autodesk Inventor professional and modified in design modeler in ANSYS package in order to study the performance of the pump in both modes as shown in Figures (5-4) and (5-5). The geometry of the flow passing through the pump was drawn by subtracting the impeller and the casing (solid bodies). The geometry is divided into four zones: pump inlet pipe, impeller, ring inlet and ring outlet. The pump inlet pipe zone refers to the flow geometry in the inlet pipe which is a stationary zone as illustrated later in this chapter. In addition, the impeller zone which refers to the flow moving between the impeller blades is a moving zone. Furthermore, the flow between the circumference of the impeller and the volute casing is divided into two main zones: the ring inlet and the ring outlet zones. The ring inlet zone was considered a moving zone as illustrated later in this chapter.

On the other hand, the pump flow was modeled using workbench as mentioned before where the pump parts were defined. The pump parts were defined as follows in workbench: Pipe inlet, Pipe outlet, impeller and volute. The volute was divided into two zones, a stationary zone and a rotating one.

Figure (5-1) pump geometry

Figure (5-2) volute casing disassembled from the pump

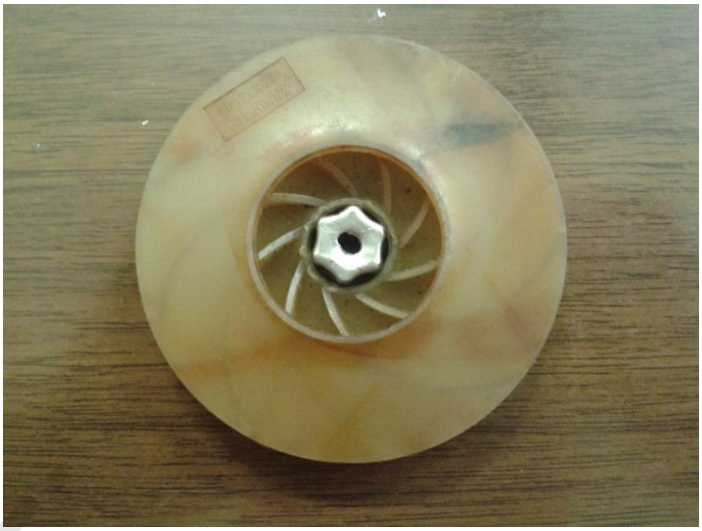

Figure (5-3) disassembled pump impeller

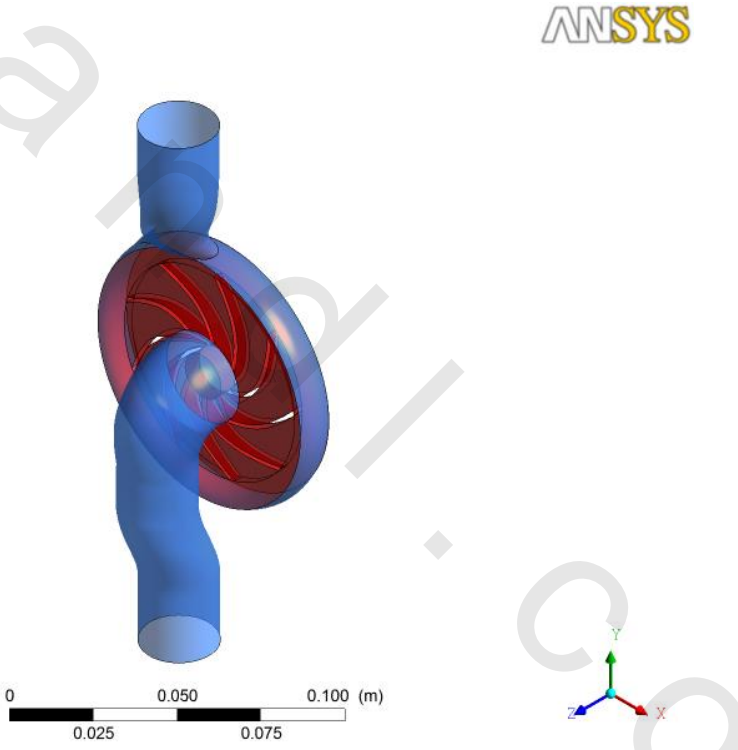

Figure (5-4) pump three-dimensional geometry

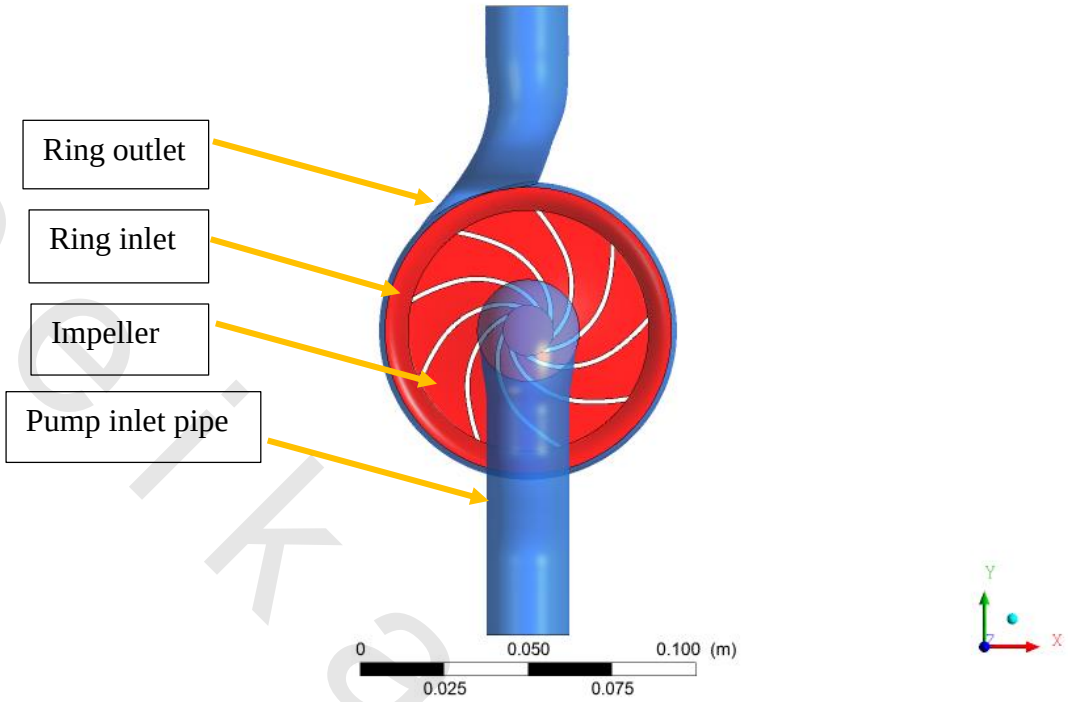

Figure (5-5) frontal view of pump three-dimensional geometry

5.3. Mesh generation

After creating the pump three-dimensional model the mesh is performed using ANSYS meshing application. The meshing parameters are detailed in Table (5-1)

Table (5-1) Meshing parameters

Meshing Parameters	**Value**
Physics Preference	CFD
Solver Preference	FLUENT
Advanced Size Function	On; Proximity and Curvature
Relevance center	Fine
Smoothing	High
Transition	Slow
Span angle center	Fine
Min size	Variable

Proximity min size	Variable
Max face size	Variable
Max size	Variable

A patch conforming method using tetrahedral elements is used in meshing direct and reverse modes of the pump. Figures (5-6 to 5-9) show different views of the mesh.

5.4 Solver

The mesh grid consists of 3000,000 cells which was found the best meshing size from the grid independence test made which is illustrated later in this chapter. The RANS (Reynolds-Averaged Navier–Stokes) model is used to solve the three-dimensional Navier Stokes equations. The multiple reference is used to solve the problem. The impeller, inner volute are rotating zones and on the other hand the pipe inlet, pipe outlet and outer volute are stationary zones.

The pressure based segregated method is applied. In this method, the governing equations are solved sequentially (i.e., segregated from one another). In the segregated algorithm, the individual Non-linear, coupled governing equations for the solution variables are solved one after another in order to obtain a converged solution. The segregated algorithm is memory-efficient, since the discretized equations need only be stored in the memory one at a time. However, the solution convergence is relatively slow, inasmuch as the equations are solved in a decoupled manner.

Different turbulence models were chosen which were recommended for turbomachinery applications. Standard & realizable k - ε, standard $k - \omega$ and Spalart –Almaras are the most suitable models for such application. The realizable k - ε is used to solve the flow as it is more accurate than the standard k - ε and RNG k - ε as it provides superior performance for flows involving rotation, boundary layers under strong adverse pressure gradients, separation, and recirculation as the case of the present study. The Realizable k - ε turbulence model is known for its robustness, economy and reasonable accuracy over a wide range of turbulent flows common in industry. The pressure-velocity coupling scheme is chosen to be SIMPLE (Semi-Implicit Method for Pressure-Linked Equations). The SIMPLE algorithm introduces pressure into the continuity equation.It relates the velocity and the pressure corrections to enforce mass conservation and to obtain the pressure field.
A least squares cell based is used in spatial discretization. In this method the solution is assumed to vary linearly. It is more beneficial to use this method on irregular (skewed and distorted) unstructured meshes as it is more accurate comparable to other methods of spatial discretization.

The PRESTO (PREssure STaggering Option) scheme uses the discrete continuity balance for a "staggered" control volume about the face to compute the "staggered" (i.e., face) pressure. This method of pressure Interpolation is more accurate for different types of meshing. A second order upwind is selected for momentum. By default, ANSYS FLUENT stores discrete values of the scalar at the cell centers. However, face values are required for the convection terms and must be

interpolated from the cell center values. This is accomplished using an upwind scheme. When second-order accuracy is desired, quantities at cell faces are computed using a multidimensional linear reconstruction approach. In this approach, higher-order accuracy is achieved at cell faces through a Taylor series expansion of the cell-centered solution about the cell centroid. Upwinding means that the face value is derived from quantities in the cell upstream, or "upwind," relative to the direction of the normal velocity. In addition, turbulent kinetic energy and turbulent dissipation rate are used in spatial discretization.

The convergence criterion was 1e-4 for the continuity. The boundary conditions are specified accurately to simulate the real case boundaries. The inlet is a pressure-inlet type and the outlet is a pressure-outlet type. The inlet is preferred to be pressure-inlet as the velocity-inlet will lead to late converged solution and more computation time than the pressure-inlet.

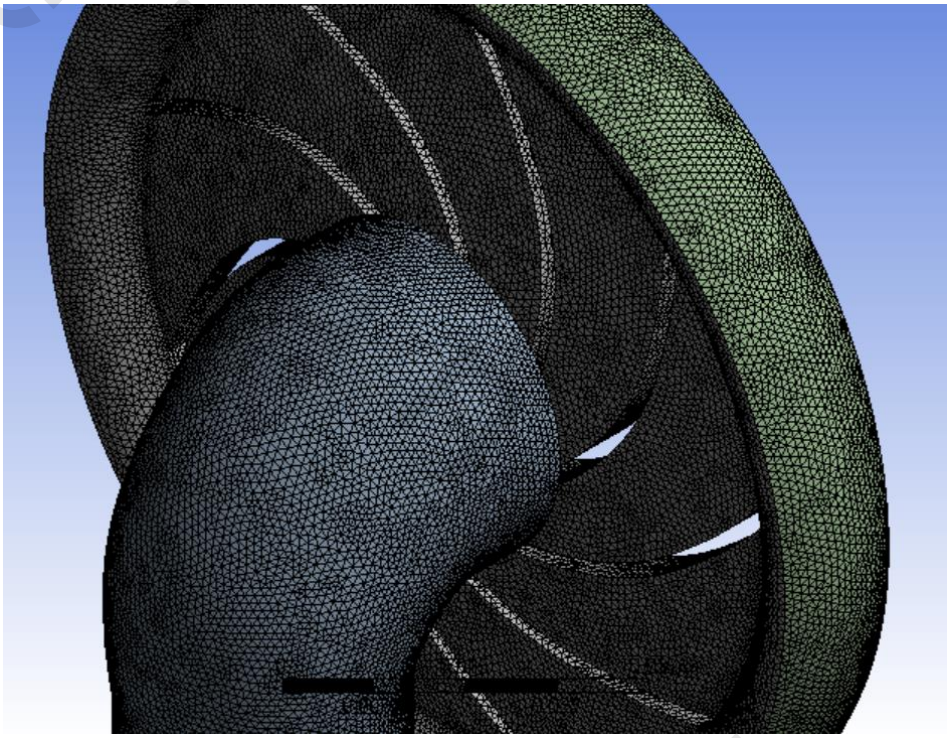

Figure (5-6) close view of the meshing

5.5. Grid Independence study

In the present study different mesh sizes are tested in order to make sure of the grid independency and to implement the most suitable one putting into consideration the computational resources and the simulation time. A grid independence test for pump and turbine modes was performed in order to choose the most suitable mesh as shown in Tables (5-2) and (5-3). The 3,000,000 cells mesh was chosen as it results in a reliable and optimized solution as concluded from the grid independence test.

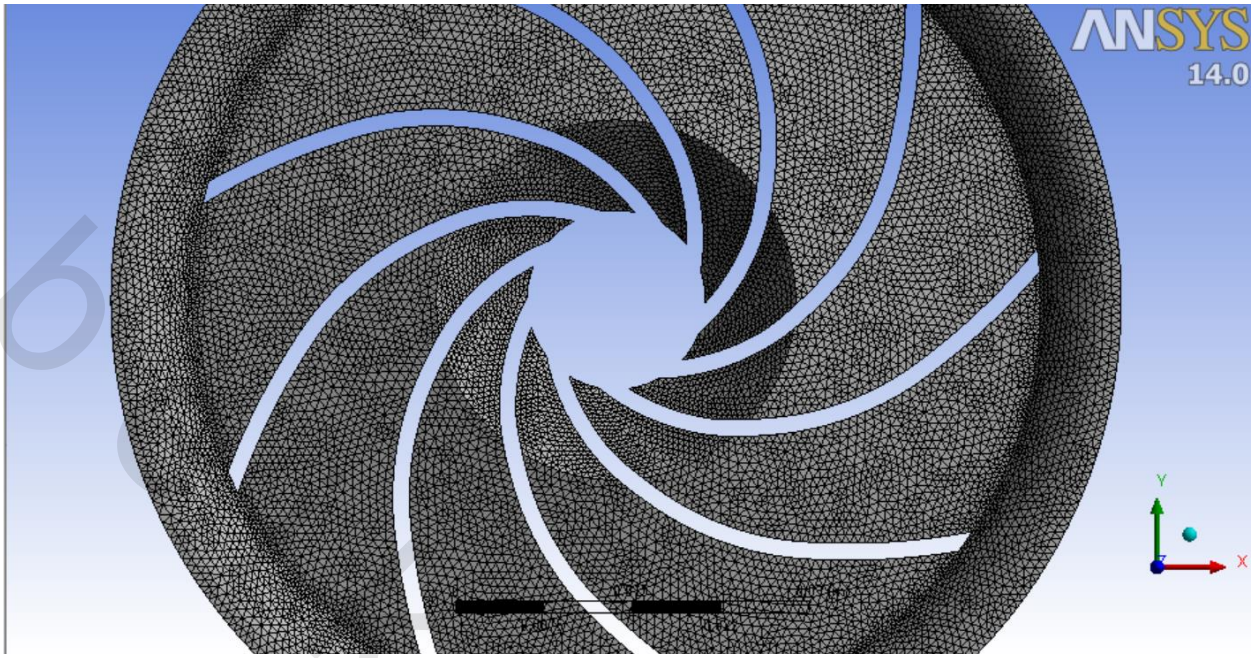

Figure (5-7) close view of the rotating zone meshing

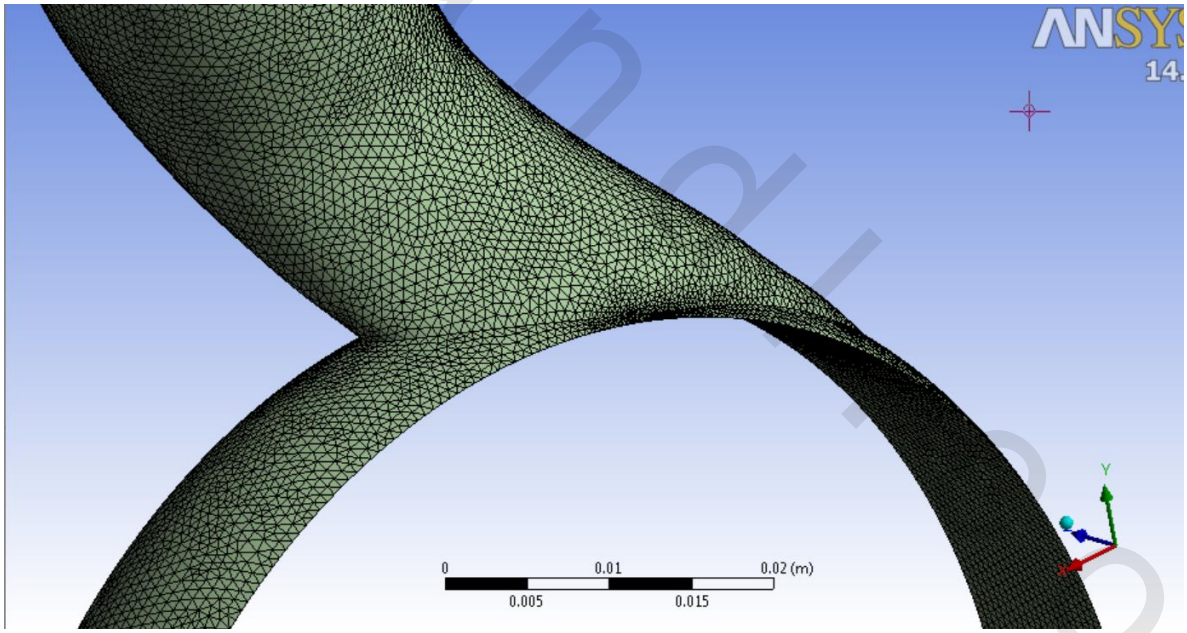

Figure (5-8) close view of the stationary zone meshing

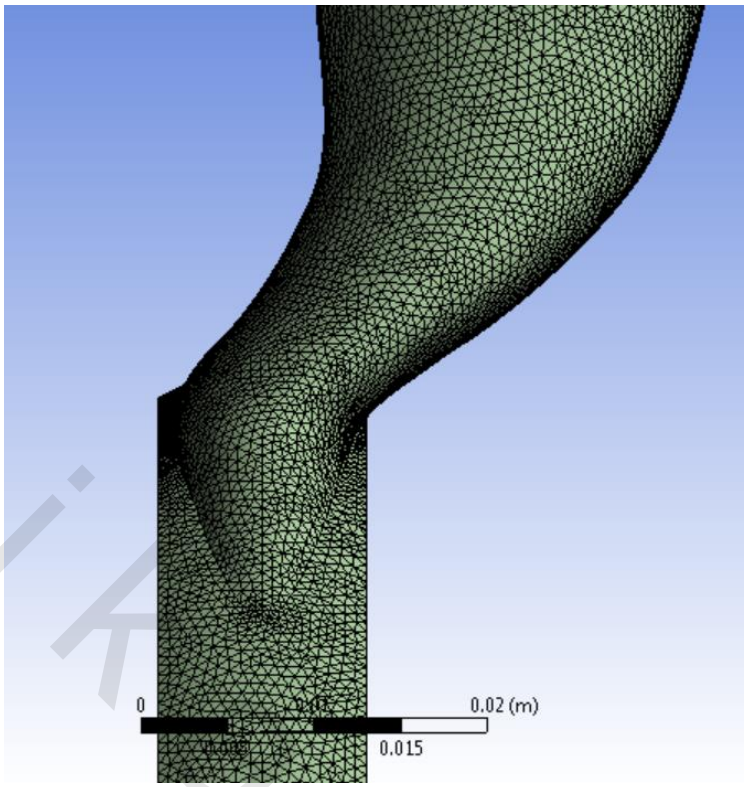

Figure (5-9) close view of the meshing in a high curvature in the pipe outlet

Table (5-2) Grid Independence study for Turbine mode

Number of cells	Mass flow rate ($\dot{m}$) kg/s	Min. residuals
500000	0.8809	1e-4
1000000	0.8722	1e-4
2000000	0.8909	1e-4
3000000	0.8893	1e-4
4000000	0.891	1e-4

Table (5-3) Grid Independence study for Pump mode

Number of cells	Mass flow rate ($\dot{m}$) kg/s	Min. residuals
1000000	0.686	1e-4
3000000	0.691	1e-4
4000000	0.704	1e-4

5.6. Ratios between Rotating and Stationary Zones

A number of different meshes were tested to determine the best ratio of the ring inlet (stationary zone) and ring outer (rotating zone) and according to [25] the more the rotating zone, the more reliable solution will be obtained, so the ratio was selected to be the highest one.

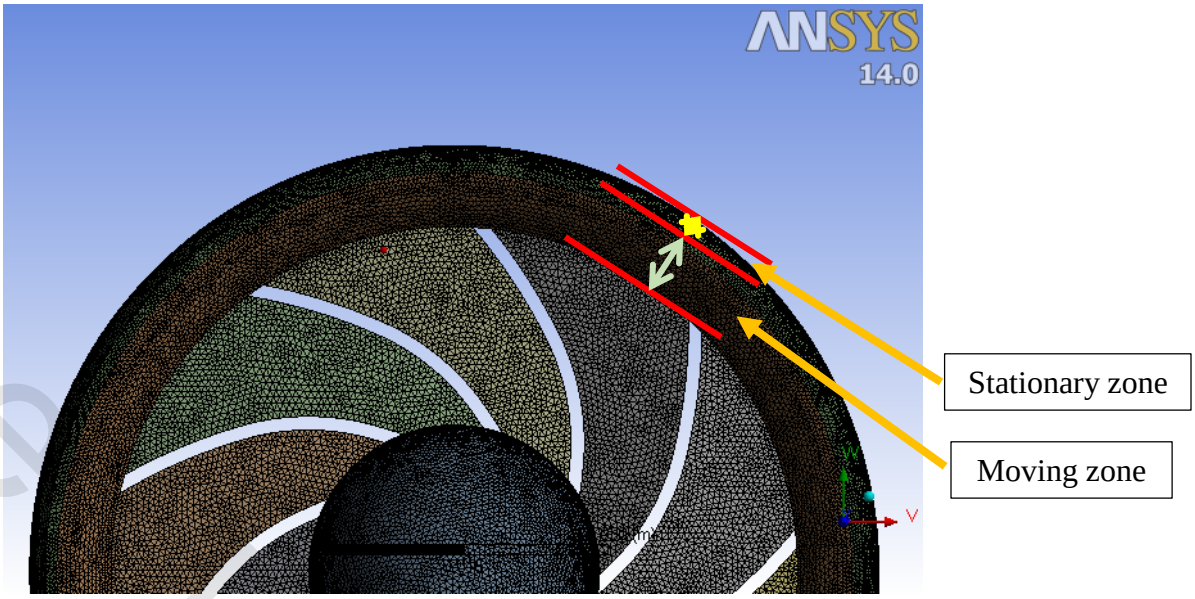

Figure (5-10) Different Ratios between moving and stationary zones

5.7. Pump Mode Results

The pump was simulated in the direct mode for different speeds of rotation. The boundary conditions in FLUENT were set to be the same as the experimental results. A pressure inlet was selected as inlet boundary condition and a pressure outlet for the outlet one as illustrated in table (5-4). These selections were based on a lot of trials in which a number of different boundary conditions were tested. The most appropriate ones were the inlet and outlet pressures as the solution is converged. Otherwise, the mass flow rate inlet and pressure outlet boundary conditions led to a non-convergent solution as the residuals didn't reach the minimum criteria which is 1e-4 so the mass inlet was not implemented. A problem encountered in the simulation results as a reverse flow appeared in the inlet and outlet of the pump as shown in Figures (5-11 to 5-13). The flow of the pump was completely reversed which means that the effect of the pump impeller rotation is not sufficient to reach the outlet pressure boundary condition (i.e. the energy difference between the inlet and the outlet are more than the manometric head given by the pump). This problem appeared as the pump real three dimensional model was not available and that the shape of outlet pipe and volute is not well defined. So, the results of the simulation was analyzed carefully in order to determine the problem arisen in the simulation results. The analysis of these results showed that there is a high velocity at the outlet from the impeller to the outlet pipe which means that the dynamic head ($v^2/2g$) didn't transferred to pressure head by the volute (i.e. the dynamic head which is not transferred to pressure head is turned to pressure loss in the volute) which means that this region is in need to be modified in order to get the real and right shape of the volute and outlet pipe. The dynamic head according to the velocity contours at 2000 RPM numerically is about 3m which corresponds to the head loss in the volute as shown in the results at Figure (5-17). It was well observed from the results in Figure (5-17) that there was a deviation from the experimental results. So, in order to overcome this problem the RPM estimation for the numerical results was changed and the RPM input was increased in FLUENT in order to determine the

relation between the experimental curve and the numerical curve. The numerical curve was found to have a 2800 RPM instead of 2000 RPM as shown in Figure (5-18). This means that lacking the exact shape of the volute and outlet pipe affects the results in a great manner. The pressure contours and the velocity contours at the BEP from the experimental results of the turbine mode at 2000 RPM is shown in Figures (5-14 to 5-16).

The pressure increases radially as illustrated in the static pressure contours in Figure (5-14) which is expected as the flow is discharged radially with the centrifugal effect and the kinetic energy is converted to pressure energy in the volute. On the other hand, the relative velocity increases radially as shown in Figure (5-16). Increasing the RPM of the motor results in shifting up the Head-Flowrate curve which is expected as the real case as the velocity which is converted to pressure head through the volute increases.

Table (5-4) boundary conditions for the BEP (pump mode)

	Inlet boundary conditions at BEP	Outlet boundary conditions at BEP
Pressure (Pa)	0.0	37396.8

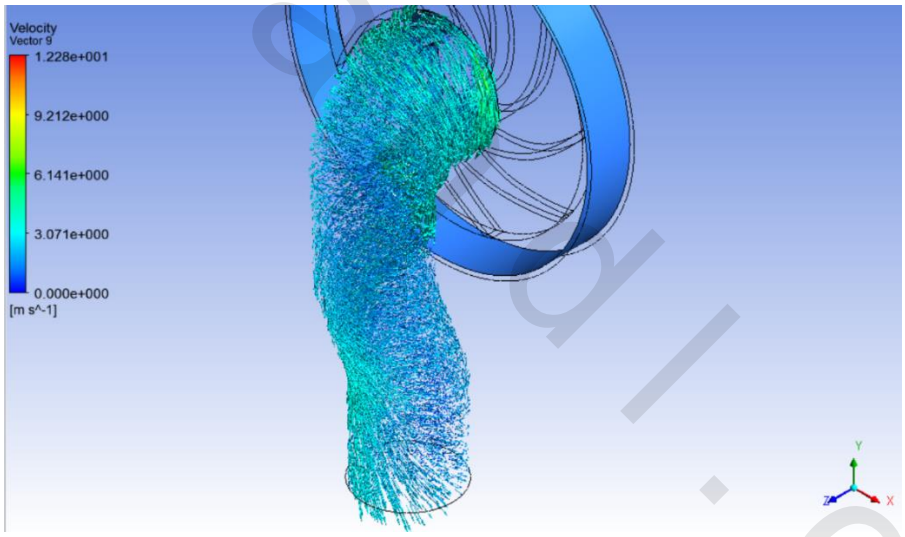

Figure (5-11) reverse flow in pump inlet pipe

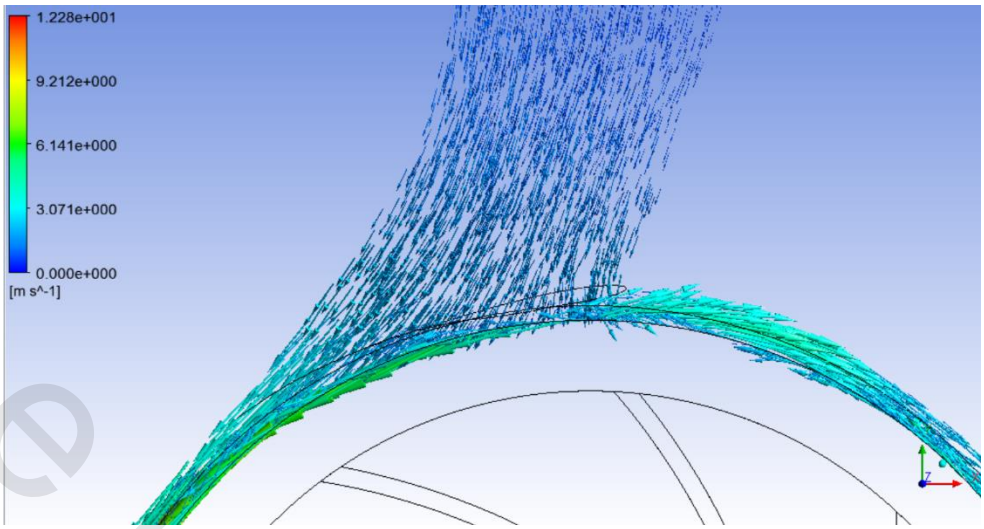

Figure (5-12) reverse flow in pump outlet pipe

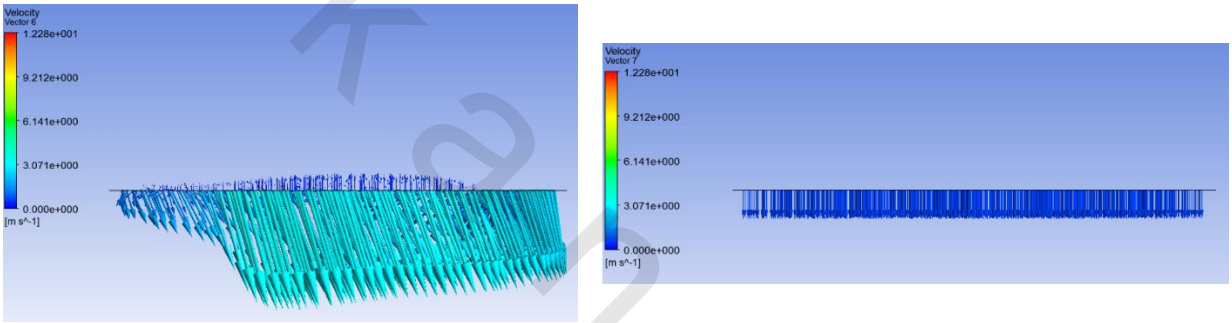

Figure (5-13) reverse flow in pump inlet and outlet sections

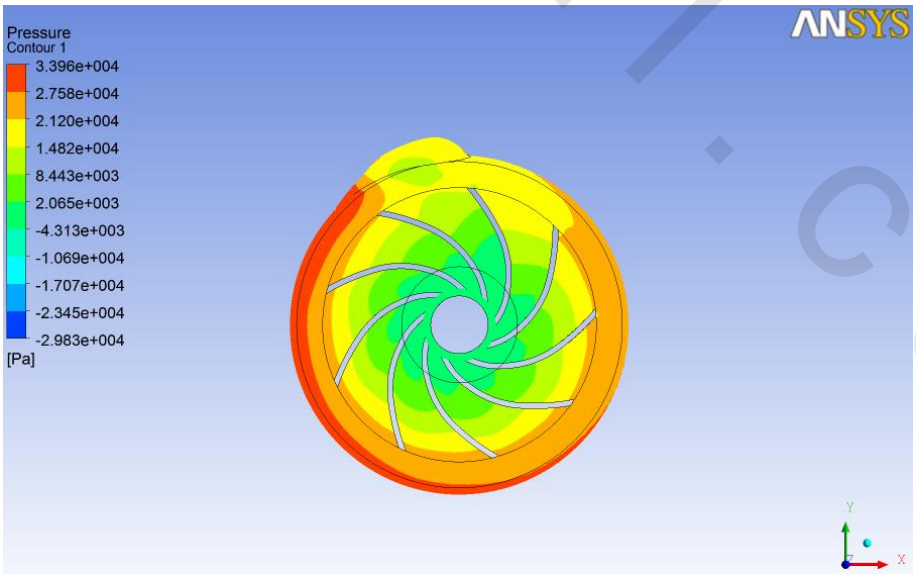

Figure (5-14) Pressure contours of a plane in the mid of the impeller thickness

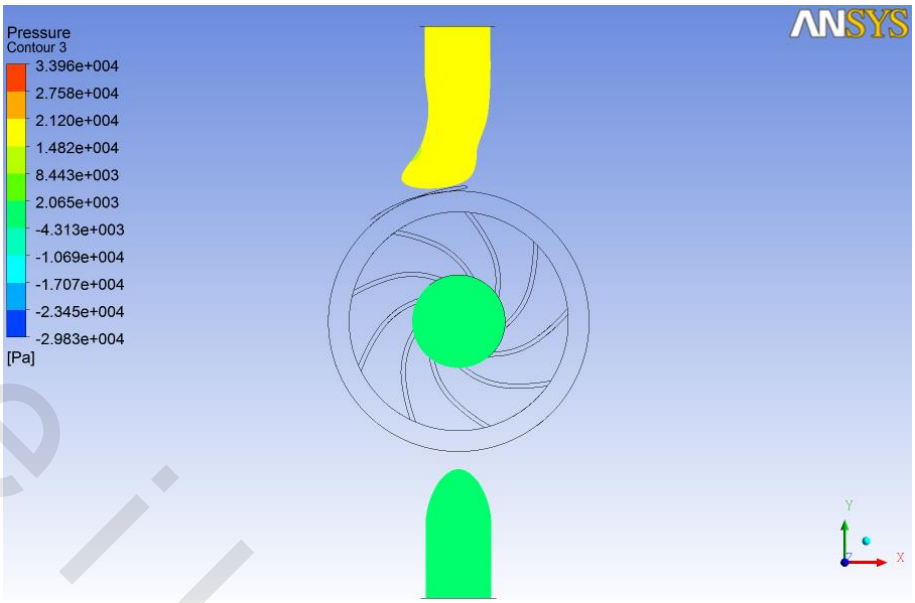

Figure (5-15) Pressure contours of a plane in the mid of the inlet and outlet pipes

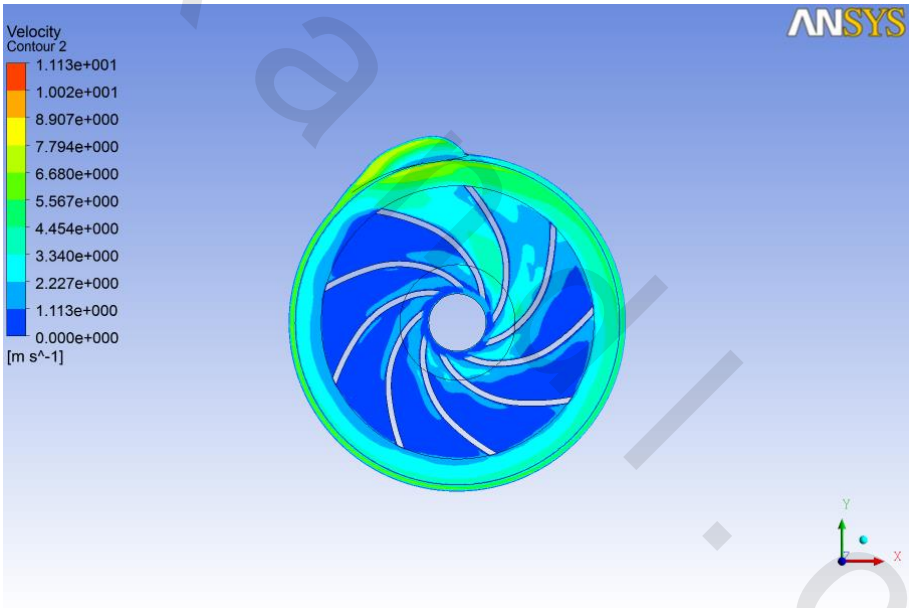

Figure (5-16) velocity contours of the mid plane in the impeller thickness

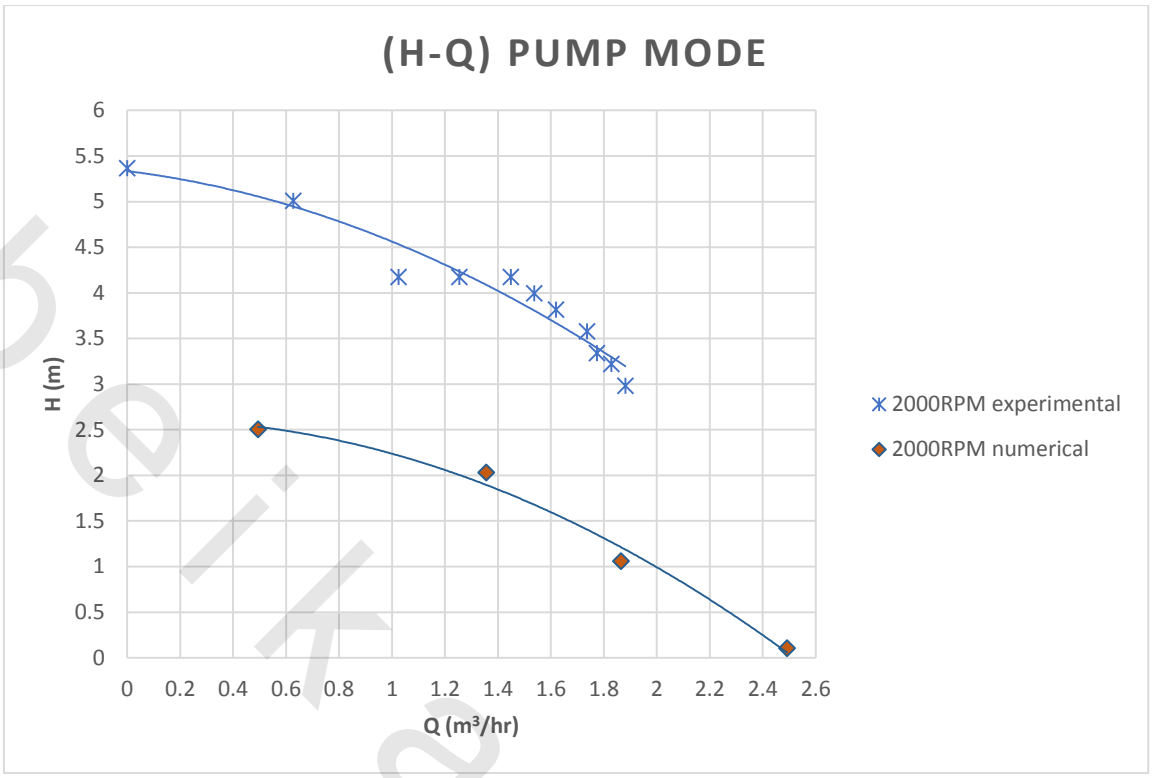

Figure (5-17) comparison between experimental and numerical curves for 2000 RPM

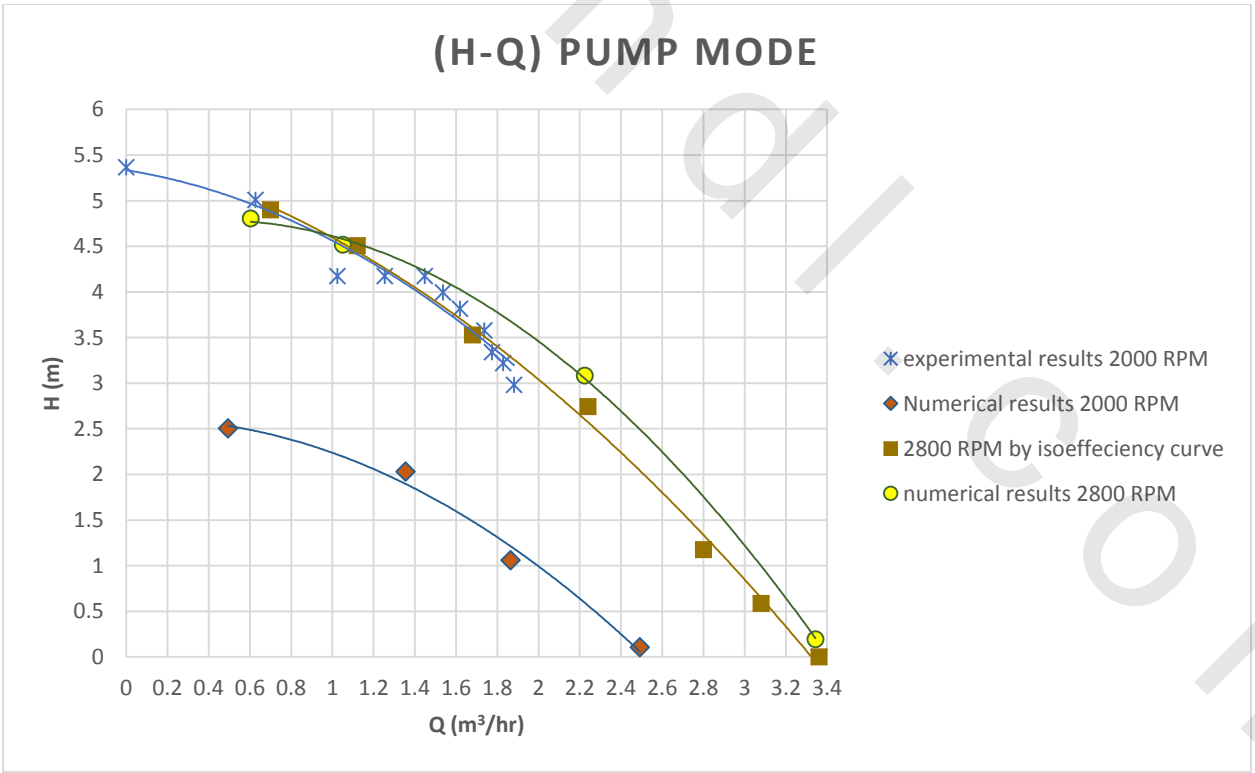

Figure (5-18) comparison between experimental curve for 2000 RPM and numerical curve for 2800 RPM and curve obtained from isoeffeciency laws for 2800 RPM

As a conclusion, simulation results have an observed difference from the experimental ones in the pump mode as illustrated in Figure (5-17). This problem arises from the lack of the pump three dimensional geometry as mentioned before. The shape of the volute and the outlet pipe affects the simulation results greatly. The angle at which the fluid exits the volute shape and enters the outlet pipe has a major effect on the results as vortices will appear if the angle deviates from the real angle by any degree. The effect of outlet pipe shape is studied as follows:

1.1.1. Effect of outlet pipe shape

The outlet pipe has a high curvature in which any change from the exact shape will simultaneously affect the simulation results. The outlet pipe shape was modified in order to get the best results from the numerical comparing to the experimental. The outlet pipe was suppressed and the results were compared with the aforementioned results as shown in Figure (5-19).

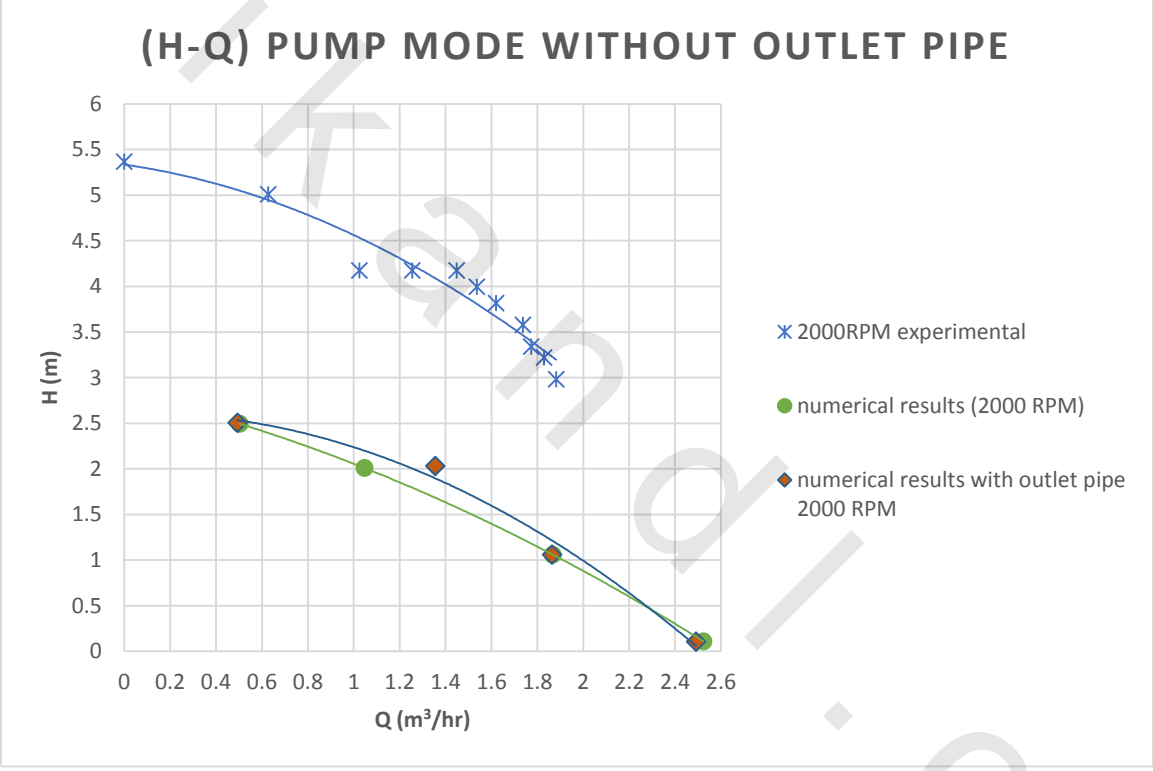

Figure (5-19) (H-Q) without outlet pipe at 2000PRM for pump mode

The results show that there is a slight change in the (H-Q) curves for the case of suppression the outlet pipe and the normal case. This means that there is a problem in the shape of the outlet pipe as there should be difference in results in both cases as the volute shape effect should be more noticeable. A number of modifications were made to the outlet pipe shape to resemble the exact shape and they are proposed to be studied.

On the other hand, one of the problems that appeared was the presence of a swirl at the inlet pipe as the shape of the inline centrifugal pump inlet differs greatly from the conventional centrifugal pump as shown in Figure (5-20). The swirl is caused by the changing of the direction of the flow to 90 degrees by a curvature as shown in Figure (5-21).

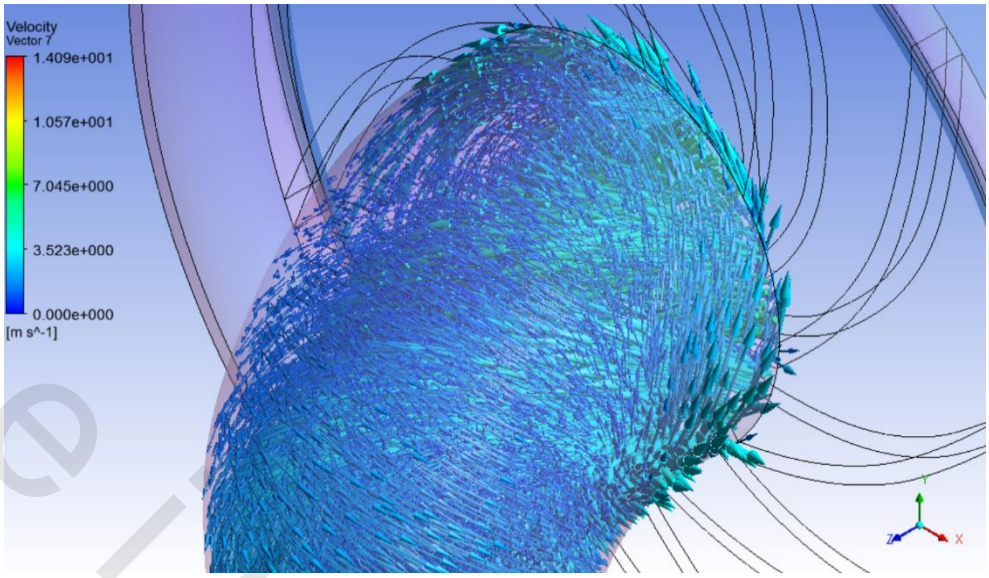

Figure (5-20) swirl at the entrance of the impeller from the inlet pipe

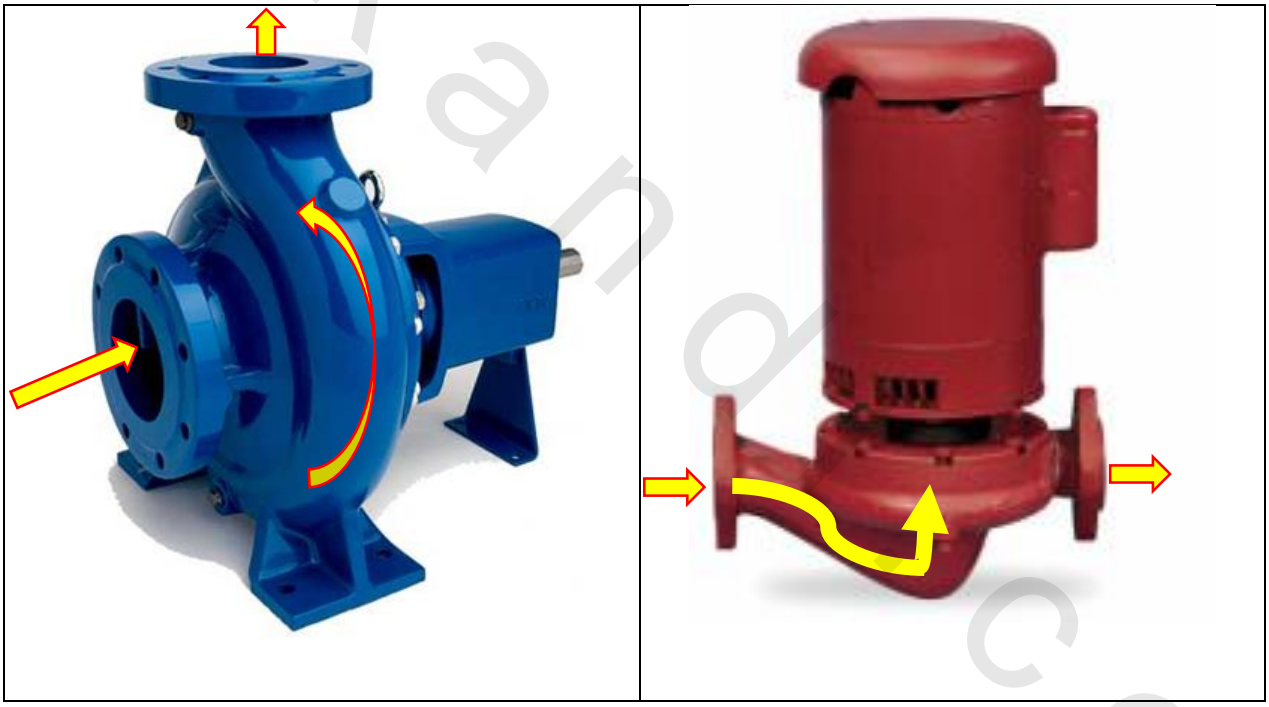

Figure (5-21) difference between flow path through conventional centrifugal pump and inline centrifugal pump

5.8. Turbine Mode Results

The pump was simulated in reverse mode as turbine for different speeds of rotation like the pump mode. The pressure contours and the velocity contours at the BEP of the turbine mode is shown in Figures (5-22 to 5-24). The boundary conditions is illustrated in Table (5-5).

Table (5-5) boundary conditions for the BEP (Turbine mode)

	Inlet boundary conditions at BEP	Outlet boundary conditions at BEP
Pressure (Pa)	62994.4	0

The aforementioned problem of Head - Flowrate curve shifting which was arisen in the pump mode didn't appear in the turbine mode case. The flow inlet and outlet was reversed from the pump case so the flow entering the turbine is directed smoothly towards the tip of the blades which decreases the deviation from the experimental results.

It is well observed from the pressure contours that the pressure decreases inward which resembles the real case. Moreover, there are some areas at the tip of the impeller where the pressure is increased as the velocity decreases dramatically in it due to circulation happened at this area. The velocity vectors in a plane in the mid of the impeller shows the circulation areas. The pressure distribution across the plane is symmetric except the near the interface between the inlet pipe and the fluid in the ring outer as shown in Figure (5-22) because of the asymmetrical shape of the inlet pipe intersection with the volute.

The velocity contours as illustrated in Figure (5-24) show that the velocity is increased with the flow direction as expected from the real case. There are some areas in which the velocity is low in the backward of the impeller due to the circulation happened in this

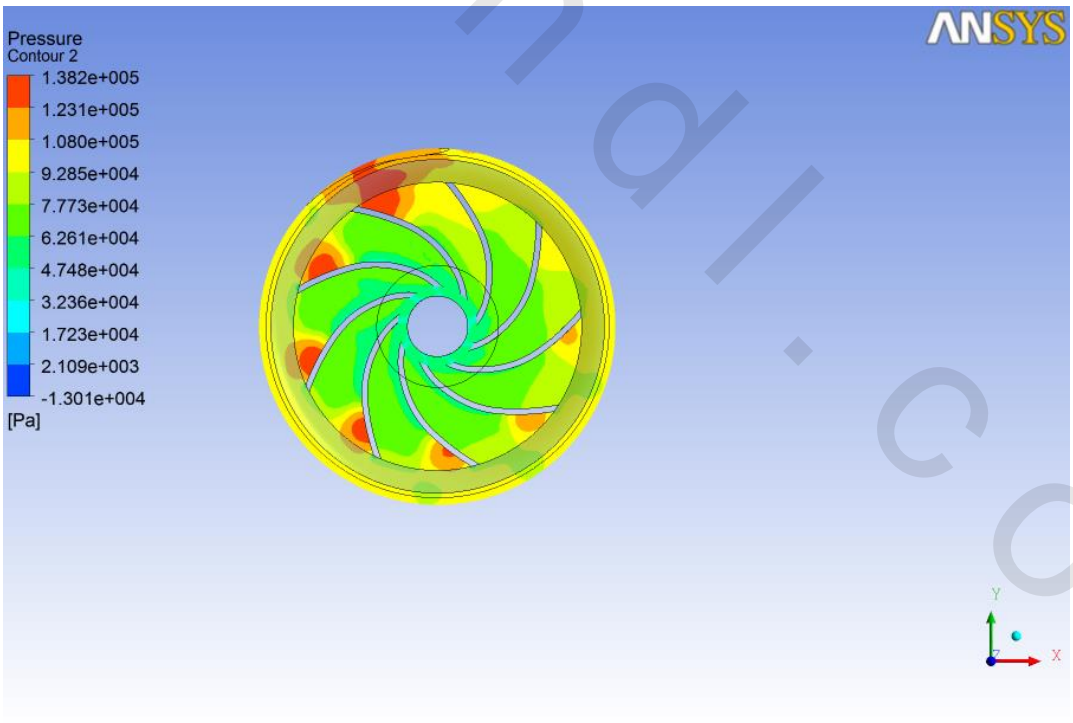

Figure (5-22) Pressure contours on a plane at the mid of the impeller thickness

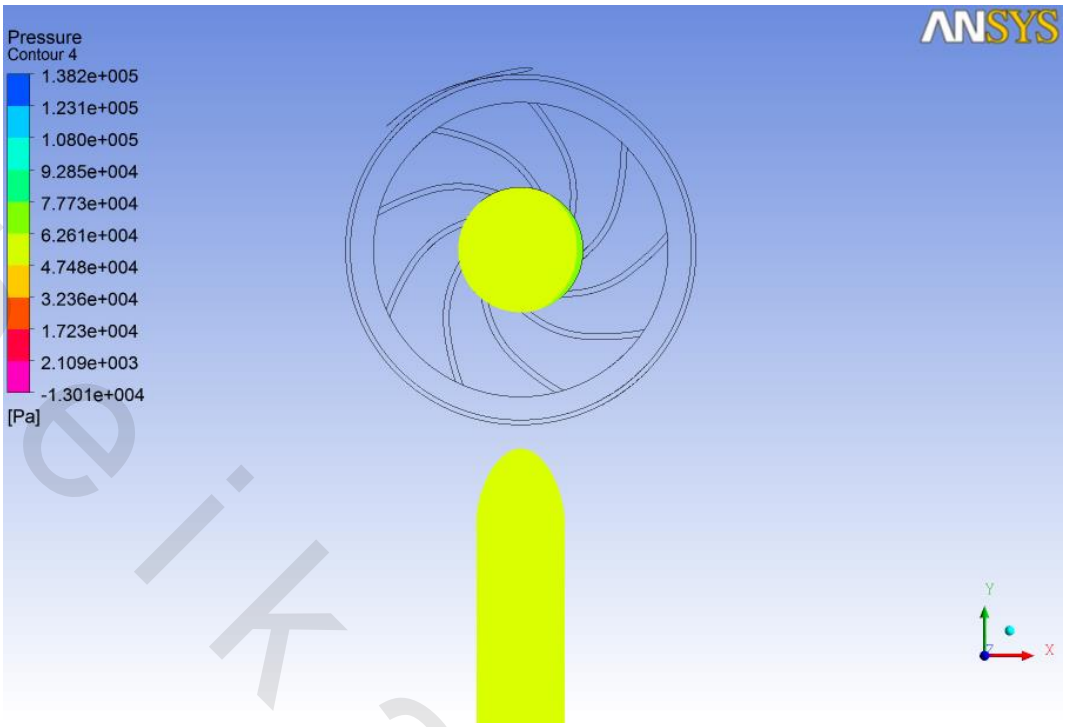

Figure (5-23) Pressure contours of a plane in the mid of the inlet and outlet pipes

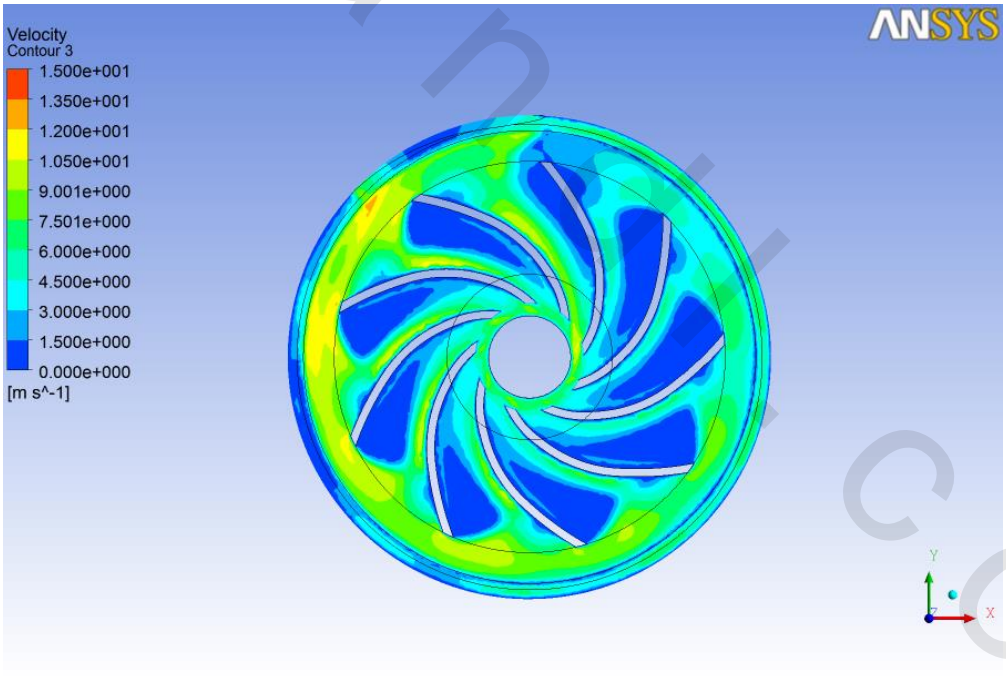

Figure (5-24) velocity contours of the mid plane in the impeller thickness

The (H-Q) characteristic curve resembles the real curve trend. As the flow rate increases the head increases as well. Comparing with the experimental results, the curve obtained from the numerical results has minor deviations from the experimental one as illustrated in Figure (5-25).

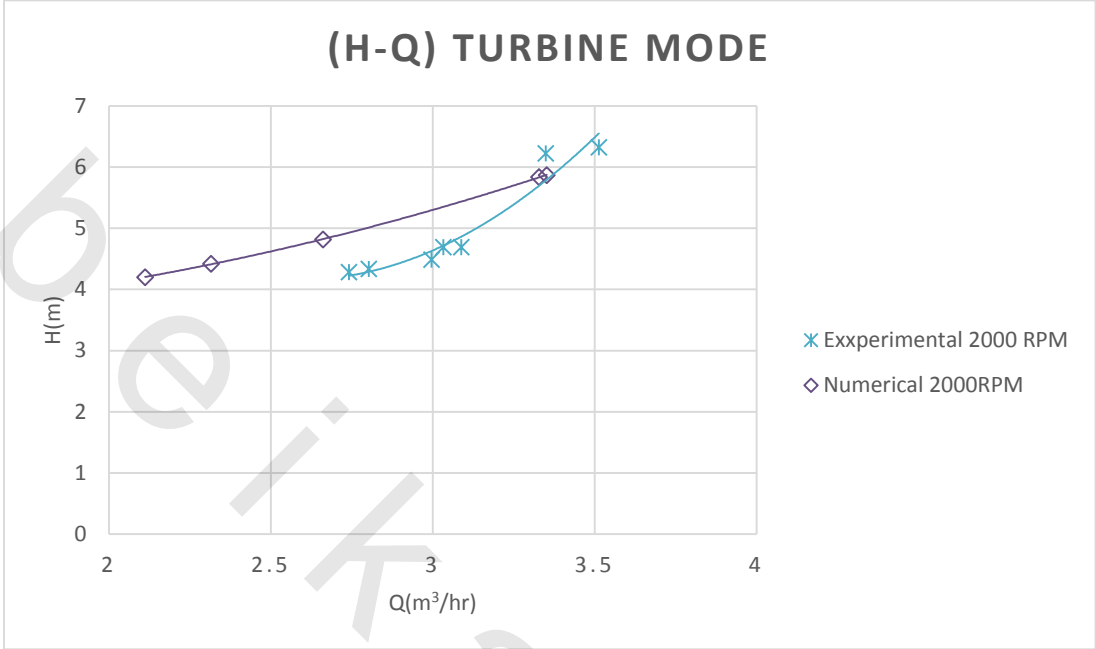

Figure (5-25) (H-Q) characteristic curve for turbine mode